

Goal-Oriented Access Optimization for ISAC-Enabled Digital Twins

Fabio Saggese, Federico Chiariotti, Shashi Raj Pandey, Henk Wymeersch, Luca Sanguinetti, Petar Popovski

Abstract—The digital twins (DTs) of physical systems and environments enable real-time remote tracking, control, and learning, but require low-latency transmission of updates and sensory data to maintain alignment with their physical counterparts. In this context, augmenting sensory data with the network’s own integrated sensing and communication (ISAC) capabilities can expand the DT’s awareness of the environment by allowing it to precisely non-radar locate measurements from mobile nodes. However, this integration increases the complexity of the communication system, and can only be supported through intelligent resource allocation and access optimization. In this work, we propose a two-step goal-oriented approach to solve this problem: we design a push-based random access in which sensors with a high Value of Information (VoI) inform the network of their access requirements, followed by a pull-based scheduled transmission of the actual sensory data. This design allows to combine the ISAC and reliable transmission requirements and maximize the VoI of the information delivered to the DT, significantly outperforming existing schemes.

I. INTRODUCTION

A digital twin (DT) of a system can enable a wide range of applications [1], being a model that replicates its dynamics and enables experiments, simulations, predictive and counterfactual analyses; however, it must be also maintained up to date with its physical counterpart in real time. This requires strict timeliness from the communication system, as well as a consideration of the most valuable information to maintain its alignment [2], so as to provide better awareness of distributed systems. This new awareness can be supported and expanded by another key technological trend in the evolution of 6G: integrated sensing and communication (ISAC) enables the communication infrastructure to simultaneously act as a sensing platform, measuring properties of the physical environment through their effects on the wireless channel [3]. The ubiquitous sensing capabilities powered by ISAC can provide a significantly expanded real-time environmental awareness.

There are still several open challenges in the design of ISAC platforms and their integration with DTs: providing efficient communication and sensing purposes services requires careful spectrum resource management [4]. Efficiently

resource allocation for the DT to remain up-to-date while guarantee good sensing performance is an even more complex problem [5]. Distributed systems such as wireless sensor networks (WSNs) add another dimension to the problem: while centralized scheduling is always a possible solution, the sensors themselves have access to the information they measure, and may have a better idea of its value to the DT application [6]. Unfortunately, at the moment, there is a dearth of effective protocols for sensing and data communication that can maintain DT models aligned with a precise localization of user equipments (UEs).

Most existing works on ISAC networks investigate joint radar and communication (JR&C) in cooperative scenarios, where a central processing unit (CPU), acting as an orchestrator, facilitates the coordination between access points (APs) [7]. The focus is on letting the JR&C algorithms feasible, accurate, and scalable [8], while the relevance of the sensing information fades into the background.

Conversely, the design of goal-oriented medium access control (MAC) and resource allocation schemes have recently seen significant developments, both adopting a distributed push-based approach [9] in which sensors themselves choose when and whether to transmit their data, and a pull-based approach in which the CPU uses its knowledge of the DT uncertainty to schedule the sensors that are expected to hold the most useful information [10]. The combination of push- and pull-based access has been discussed in [11], showing that there are significant coexistence gains from integrating the two approaches in DT scenarios. However, to the best of our knowledge, goal-oriented access schemes have only considered in communication, without any ISAC capabilities.

This work fills this gap by proposing a joint goal-oriented design of communication and localization resource allocation: we consider a frame structure divided in two subframes, which allows for sensors with important information to proactively report their Value of Information (VoI) and communication requirements in a *push subframe*, followed by a *pull subframe* [11] in which the AP can optimize resource allocation to maximize the total VoI while respecting localization requirements, in terms of a maximum position error bound (PEB). We design a protocol that includes both the grant-free access in the push subframe and the scheduling optimization in the pull subframe and provide an analytical bound for communication and localization performance. Our simulations show that our approach enables the integration of DTs and ISAC, significantly outperforming existing VoI-unaware schemes and approaching oracle-based upper bounds.

F. Saggese (fabio.saggese@ing.unipi.it) and L. Sanguinetti (luca.sanguinetti@unipi.it) are with the Dept. of Information Engineering, University of Pisa, Italy. F. Chiariotti (federico.chiariotti@unipd.it) is with the Dept. of Information Engineering, University of Padova, Italy. H. Wymeersch (henkw@chalmers.se) is with the Dept. of Electrical Engineering, Chalmers University of Technology, Sweden. S. R. Pandey and P. Popovski ({srp,petarp}@es.aau.dk) are with the Dept. of Electronic Systems, Aalborg University, Denmark. F. Saggese work is funded by Horizon Europe MSCA Postdoctoral Fellowships, grant 101204088. Velux Foundation, Denmark, through the Villum Investigator Grant WATER, nr. 37793, and by the Horizon Europe SNS “6G-GOALS” project, grant 101139232 supported this work.

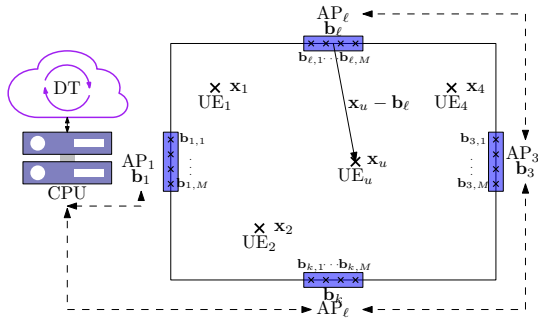


Fig. 1: Example of the scenario.

II. SYSTEM MODEL

We consider the 2D WSN scenario shown in Fig. 1, with L APs, each equipped with a M -antenna uniform linear array (ULA), and U single-antenna mobile UEs. The APs are connected through an out-of-band channel to a CPU running a DT of the system.

Assuming a common frame of reference, the position of the antennas of the ℓ -th AP is denoted as $\mathbf{B}_\ell = [\mathbf{b}_{\ell,m}]_{m \in \mathcal{M}} \in \mathbb{R}^{2 \times M}$, while its center is $\mathbf{b}_\ell = \frac{1}{M} \mathbf{1}_M^T \mathbf{B}_\ell$. The system works in a *frame-based* fashion, designed so that the position of each UE, denoted as $\mathbf{x}_u \in \mathbb{R}^2, \forall u \in \mathcal{U} = \{1, \dots, U\}$, can be approximated as constant throughout the frame. The UEs have different sensors on board, used to collect sensing data while moving throughout the environment with a maximum velocity v_u . The aim of each node is to send *relevant* sensing data to the APs through a wireless channel.

A. Application model

The relevance of observations for the DT is assessed through the VoI. The normalized VoI of a user u is an independent and identically distributed (i.i.d.) random variable denoted as $V_u \in [0, 1]$ characterized by its cumulative distribution function (CDF) P_v , and we assume that UE u can locally obtain the value of V_u [9]. Additionally, all UEs know P_v .

We further assume that the non-radar observations obtained by the UEs have a considerable size. The observation size for each node, measured in bytes, is an i.i.d. random variable B_u , and it requires significant physical resources to transmit. Therefore, we consider a two-step system: first, the UEs employ a *push* paradigm to inform the CPU about their data size and VoI, then wait to be *pulled* for the actual data transmission, avoiding contention when transmitting data that span multiple packets. Every transmission attempt in the push subframe indicates that UE's update has a high VoI.

While the CPU takes care of processing the receiving signals, it also needs to estimate the position of the UEs to link the received information to a specific location in the environment and update the DT accordingly. Therefore, the CPU will schedule spectrum resources so as to maximize the total VoI, i.e., optimize communication in a goal-oriented fashion,

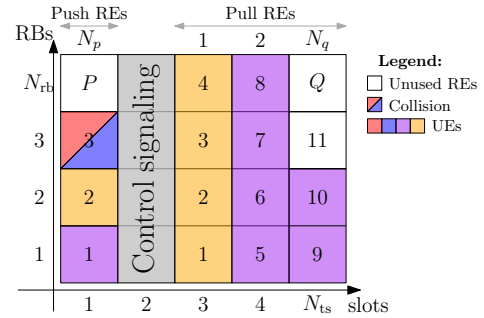


Fig. 2: Example of the resource grid for a frame

ion, while targeting a PEB as a proxy metric for localization performance.¹

B. Frame-based OFDM resource grid

Each frame is subdivided into downlink (DL) and uplink (UL) portions: the former is used by the AP for control signaling, which is assumed to be ideal throughout the paper, while the latter is reserved for UE transmissions, as shown in Fig. 2. The frame follows an underlying orthogonal frequency division multiplexing (OFDM) structure through a time-frequency resource grid of N_{ts} time slots and N_{rb} resource blocks (RBs). A single slot-RB is the smallest indivisible unit of resources that can be scheduled, and is referred as a resource element (RE). It comprises F subcarriers spaced by Δ_F [Hz] and T OFDM symbols with cyclic prefix (CP) duration of T_{cp} [s], assumed longer than channel delay spread.

The frame is further subdivided in two subframes. The *push subframe* occupies the first N_p slots and N_{rb} RBs, for a total of $P = N_p N_{rb}$ REs. The UEs having relevant data will demand resources by attempting access within the push subframe by transmitting a packet in a Framed Slotted-Aloha (FSA) fashion, as discussed in Sec. III-A. This packet only contains the current VoI, V_u , and the observation size, B_u , and thus it may be transmitted in a single RE. After decoding the packets in the push subframe, the AP is able to find a scheduling policy satisfying the communication and localization criteria through the procedure presented in Sec. III-C.

The *pull subframe* occupies N_q time slots and N_{rb} RBs, for a total of $Q = N_q N_{rb}$ REs, with $Q \geq P$. The scheduled UEs employ the REs for the transmission of the relevant data, while the AP exploits the channel estimates in those REs to perform positioning on the transmitting UE, as discussed in Sec. III-B. We denote as \mathcal{P} and \mathcal{Q} the set containing the indexes of the REs of the push and pull subframes, respectively.

The *control signaling* portion occupies the remaining time slots between the two subframes, and it is used for *broadcasting* the schedule for the pull subframe.

C. PHY layer modeling

We assume perfect synchronization between the AP's local oscillators (LOs) [8], [12]. The UEs perform synchronization

¹Root mean square error performance may be worse; the PEB is used to abstract from a specific localization method and its tractability.

employing the 5G new radio (NR) standard procedure on the physical random access channel (PRACH) [13]. compensating their LO up to a residual. The residual frequency offsets (FOs) caused by carrier frequency offset (CFO) and the Doppler effect is considered negligible due to 1) higher precision for CFO compensation [14], 2) low speed v_u , and 3) positioning focus. Conversely, we denote the residual clock timing offset (CTO) of UE $u \in \mathcal{U}$ at REs as $\delta\tau_u$, assumed to be approximately constant throughout the frame.

For the channel modeling, let us consider a single RE, i , and a single UE, $u \in \mathcal{U}$. The sets indexing the subcarriers and the OFDM symbols in RE i are \mathcal{F}_i and \mathcal{T}_i . We assume a line-of-sight (LOS) dominant channel model. Thus, the (concatenation of the) UL channel vectors between UE u and the L AP ℓ varies only over the subcarriers and is given by [15], [16]:

$$\mathbf{h}_{u,i} = \sum_{\ell \in \mathcal{L}} \sqrt{\beta_{u,\ell}} e^{j\psi_{u,\ell}} (\mathbf{e}_\ell \otimes \mathbf{f}_{u,\ell,i} \otimes \mathbf{a}_{u,\ell}) \in \mathbb{C}^{LFM}. \quad (1)$$

where $\mathbf{e}_\ell = [\mathbf{0}_{\ell-1}^\top, 1, \mathbf{0}_{L-\ell}^\top]^\top \in \mathbb{R}^L$; $\beta_u = [\beta_{u,\ell}]_{\ell \in \mathcal{L}}$ is the large scale fading, and $\psi_u = [\psi_{u,\ell}]_{\ell \in \mathcal{L}}$ is the phase offset [15]; vector $\mathbf{f}_{u,\ell,i} \in \mathbb{C}^F = [\exp(-j2\pi f \Delta_F \tau_{u,\ell})]_{f \in \mathcal{F}_i}^\top$ accounts for the effect of delay due to propagation and CTO, $\tau_{u,\ell} = \|\mathbf{x}_u - \mathbf{b}_\ell\|_2 / c + \delta\tau_{u,\ell}$, with c being the speed of light; $\mathbf{a}_{u,\ell} \in \mathbb{C}^F = [\exp(j\frac{2\pi}{\lambda} (\mathbf{b}_{\ell,m} - \mathbf{b}_\ell)^\top (\mathbf{x}_u - \mathbf{b}_\ell) / \|\mathbf{x}_u - \mathbf{b}_\ell\|_2)]_{m \in \mathcal{M}}$ is the steering vector with λ being the wavelength.

The signal received for a singleton RE is

$$\mathbf{Y}_i \in \mathbb{C}^{LFM \times T} = \sqrt{p_u} \mathbf{h}_{u,i} (\mathbf{1}_{LM} \otimes \mathbf{S}_{u,i}) + \mathbf{W}_i, \quad (2)$$

where $\mathbf{S}_{u,i} \in \mathbb{C}^{F \times T}$ is the block of transmitted symbols with $\mathbb{E}[\mathbf{S}_{u,i}] = \mathbf{0}_{F \times T}$ and $|(\mathbf{S}_{u,i})_{t,f}|^2 = 1$; p_u is the transmission power of UE $u \in \mathcal{U}$; $(\mathbf{W}_i)_{t \in \mathcal{T}} \sim \mathcal{CN}(\mathbf{0}_{LM}, \sigma_w^2 \mathbf{I}_{LMF})$ is the additive white Gaussian noise (AWGN) of the APs.

To perform channel estimation (CE) at the AP side, each first OFDM symbol in the RE, $(\mathbf{S}_{u,i})_{:,1}$, carries a known pilot symbol. Employing least-squares (LS) estimation yields [12]

$$\hat{\mathbf{h}}_{u,i} = p_u^{-\frac{1}{2}} (\mathbf{Y}_i)_{:,1} \odot (\mathbf{S}_{u,i}^*)_{:,1} = \mathbf{h}_{u,i} + \tilde{\mathbf{w}}_i \quad (3)$$

where $\tilde{\mathbf{w}}_i = (\mathbf{W}_i)_{:,1} / \sqrt{p_u} \sim \mathcal{CN}(\mathbf{0}_{LFM}, \frac{\sigma_w^2}{p_u} \mathbf{I}_{LFM})$. We remark we assumed that only a UE transmits on the same RE; if a collision occurs on RE within the push subframe $i \in \mathcal{P}$, the CE is unfeasible due to pilot contamination and the data transmitted in the RE is lost.² Conversely, within the pull subframe, scheduling is made in an orthogonal manner preventing pilot contamination—see Sec. III-B.

III. GOAL-ORIENTED ACCESS DESIGN

This section outlines the design strategies to maximize the total VoI per frame. The proposed approach ensure a per-UE reliable delivery of the sensory data of size B_u , and a PEB of at least ϵ by allocating the Q REs within the pull subframe.

A. Push subframe strategy

The UEs apply a threshold policy during the push subframe, transmitting a message over a randomly selected RE among

²This is the worst-case scenario: due to the capture effect, data from UEs with favorable propagation conditions may still be decoded.

\mathcal{P} if $V_u > \theta$, which maximizes the expected VoI under our assumptions [9]. As all UEs have the same threshold, the transmission probability of each UE is $1 - P_v(\theta)$, and the probability that n UEs will attempt to reserve resources is

$$p_{\text{tx}}(n|\theta) = U!(n!(U-n)!)^{-1} P_v(\theta)^{U-n} (1 - P_v(\theta))^n. \quad (4)$$

Following the signal model in the previous section, we consider the success probability for two or more UEs colliding over the same RE to be negligible, and the erasure probability for a singleton RE, i.e., an RE over which a single UE transmits, to also be negligible.

We define $\mathcal{C}(k, n) = \{\mathbf{c} \in \mathbb{Z}^k : c_i \geq 2 \forall i \wedge \sum_{i=1}^k c_i = n\}$ as the set of possible combinations of n UEs colliding over k REs. The probability of having s singleton REs and c collided REs, given that n nodes transmit, is then

$$p_o(s, c|n) = \begin{cases} \frac{\binom{n}{s} \sum_{\mathbf{k} \in \mathcal{C}(c, n-s)} \binom{n-s}{\mathbf{k}} P!}{P^n (P-s-c)! c!}, & c > 0, n \geq s + 2c; \\ \frac{P!}{P^s (P-s)!}, & c = 0, s = n; \\ 0, & \text{otherwise.} \end{cases} \quad (5)$$

where $\binom{n-s}{\mathbf{k}}$ is the multinomial coefficient. Naturally, the maximum value of s is P . The probability of s successful transmissions can then simply computed using the law of total probability as $p(s|\theta) = \sum_{n=s}^U \sum_{c=0}^{\min(\frac{n-s}{2}, P-s)} p_o(s, c|n) p_{\text{tx}}(n|\theta)$. It is thus possible to optimize the push subframe. Regardless, we denote the set of UEs that transmits successfully as $\mathcal{S} \subseteq \mathcal{U}$.

B. Per-UE allocation for system performance guarantees

Once the push subframe is over, the CPU decodes the received packets obtaining V_u and B_u , $\forall u \in \mathcal{S}$, used to perform RE assignment. Here, we analyze how to evaluate the minimum amount of REs per UE, namely Q_u , to satisfy the communication and localization constraints.

Communication: The aim is obtaining the amount of resources Q_u^{com} guaranteeing an achievable rate when UE $u \in \mathcal{S}$ transmits B_u bytes. Due to the orthogonal allocation, UE's transmitted symbols are estimated employing maximum ratio (MR) combining to \mathbf{Y}_i , i.e., the APs' combiner vectors is $\mathbf{v}_i = \hat{\mathbf{h}}_{u,i}$. Using the *use-and-then-forget (UatF) bound*, the effective achievable spectral efficiency (SE) for a single (f, t) in the RE is [12, Th. 5.2]

$$\rho_u(\beta_u) = \log \left(1 + \frac{p_u}{\sigma_w^2} \frac{M \left| \sum_{\ell \in \mathcal{L}} \beta_{u,\ell} \right|^2}{2 \sum_{\ell \in \mathcal{L}} \beta_{u,\ell} + \frac{\sigma_w^2}{p_u} L} \right), \quad [\text{bit/s/Hz}]. \quad (6)$$

To deliver a packet of B_u bytes, UE $u \in \mathcal{S}$ thus needs

$$Q_u^{\text{com}} \geq 8B_u (\rho_u(\beta_u) (T-1)F)^{-1}. \quad (7)$$

We employ an energy detector (ED) on the channel estimate obtained in the push subframe to estimate β_u . Denoting $i^* \in \mathcal{P}$ as the RE in which UE $u \in \mathcal{S}$ transmitted within the push subframe, we have

$$\hat{\beta}_u = \frac{1}{FM} \sum_{\ell \in \mathcal{L}} \|\mathbf{e}_\ell^\top \hat{\mathbf{h}}_{u,i^*}\|_2^2 \mathbf{e}_\ell \approx \beta_u + \frac{\sigma_w^2}{p_u TFM} \chi_{FM}^2 \quad (8)$$

with $\chi_{FM}^2 \in \mathbb{R}^L$ being a Chi-squared distributed vector with FM degrees of freedom. Therefore, the number of pull subframe's REs UE $u \in \mathcal{U}$ satisfying the communication constraints is³

$$Q_u^{\text{com}} = \left\lceil 8B_u(\rho_u(\hat{\beta}_u)(T-1)F)^{-1} \right\rceil. \quad (9)$$

Localization: The aim is obtaining the amount of resources Q_u^{loc} guaranteeing a PEB $\leq \epsilon$ for all UEs $u \in \mathcal{S}$. Denoting the set indexing Q_u^{loc} as \mathcal{Q}_u , the squared PEB (SPEB) is given by $\text{PEB}_u^2 = \text{tr}[(\sum_{i \in \mathcal{Q}_u} \mathbf{J}_i)^{-1}]_{1:2;1:2}$ being \mathbf{J}_i the Fisher information matrix (FIM) for RE i over the vector $\boldsymbol{\kappa}_u = [\mathbf{x}_u^T, \boldsymbol{\beta}_u^T, \boldsymbol{\psi}_u^T, \delta\tau_u]^T \in \mathbb{R}^{2L+1}$ collecting the location and nuisance parameters of UE $u \in \mathcal{U}$. It can be bounded by

$$\text{PEB}_u^2 \leq \text{tr} \left[(Q_u^{\text{loc}} \mathbf{J}_1)^{-1} \right]_{1:2;1:2} \leq \epsilon^2, \quad (10)$$

by neglecting the delay accuracy gain provided by scheduling over higher bandwidths [17], and yielding

$$Q_u^{\text{loc}} = \left\lceil \epsilon^{-2} \text{tr}[(\mathbf{J}_1)^{-1}]_{1:2;1:2} \right\rceil. \quad (11)$$

To compute the FIM, we remark that localization method occurs after data decoding, letting use the retrieved symbol $\mathbf{S}_{u,i}$ as pilot by applying eq. (3) to all the OFDM symbols. Thus, we have T independent copies of the estimated channel $\hat{\mathbf{h}}_{u,i} \sim \mathcal{CN}(\mathbf{h}_{u,i}, \frac{\sigma_w^2}{p_u} \mathbf{I}_{LFM})$, yielding [18]

$$\mathbf{J}_i = 2T \frac{p_u}{\sigma_w^2} \Re \left\{ \nabla_{\boldsymbol{\kappa}_u} \mathbf{h}_{u,i}^H \nabla_{\boldsymbol{\kappa}_u} \mathbf{h}_{u,i} \right\} \quad (12)$$

where the gradients are given in the Appendix, depending on \mathbf{x}_u , and $\boldsymbol{\beta}_u$. To approximate them, we use $\hat{\boldsymbol{\beta}}_u$ in (8), and the worst-case position $\tilde{\mathbf{x}}_u = \arg \min_{\mathbf{x}} \text{tr}[(\mathbf{J}_1(\mathbf{x}, \hat{\boldsymbol{\beta}}_u)^{-1})_{1:2;1:2}]$, found by grid-search. Due to eq. (1), $\tilde{\mathbf{x}}_u$ depends on \mathbf{B}_ℓ only, leading to a single grid-search per scenario.

The minimum amount of REs per UE satisfying both communication and localization constraints is therefore

$$Q_u = \max\{Q_u^{\text{com}}, Q_u^{\text{loc}}\}. \quad (13)$$

C. Pull subframe scheduling strategy

Let us now schedule the pull subframe. We denote as $g_i \in \mathcal{U}$ the scheduling variable indicating which UE $u \in \mathcal{U}$ RE $i \in \mathcal{Q}$ is assigned to for data transmission in the pull subframe, cf. Sec. II-B. UE u has a minimum allocation Q_u , required to satisfy both communication and localization constraints, given in (13). The utility for the CPU from scheduling UE u is then equal to V_u if both constraints are satisfied and 0 otherwise. Furthermore, only UEs that managed to transmit during the push subframe, i.e., $u \in \mathcal{S}$, have communicated their VoI, and are thus eligible for scheduling. We then pose the following optimization problem:

$$\mathbf{g}^* = \arg \max_{\mathbf{g} \in \mathcal{U}^{\mathcal{Q}}} \sum_{u \in \mathcal{S}} V_u I \left(\sum_{i \in \mathcal{Q}} I(g_i = u) \geq Q_u \right), \quad (14)$$

³The approximation is tight for high TFM , which is usually the case. The ED noise may make the rate unachievable, but the use of the UatF bound and high FTM value, the chances of this occurrence are negligible.

where $I(a) = 1 \iff a$ is true. This is an instance of the knapsack problem, which belongs to the NP-Hard class, and there are no known polynomial-time optimization algorithms. We then use a heuristic approach: *a)* we first solve the continuous relaxation of the problem by sorting the UEs by their value per RE, $\frac{V_u}{Q_u}$, and assign the requested REs to the first UEs that avoids overflow; then, *b)* we adopt a *remove-one local search heuristic*, removing one element from the solution and checking if it leads to an improvement, until the solution is stable. While this heuristic have an optimality gap, this should be relatively small in practical scenarios, and it can be run in real time by the CPU.

IV. SIMULATION SETTINGS AND RESULTS

We perform numerical simulations considering a square scenario with a side of 200 m, where the APs and their antennas are symmetrically positioned with antenna spacing $\lambda/2$. Each simulation contains 100 frames; the UEs are randomly positioned and then move following Brownian motion. Large-scale fading β_u is evaluated through free-space path loss (FSPL) with gain 2.15 dBi. The results are averaged over 10^4 episodes. The simulation parameters are given in Tab. I.⁴

We compare the performance of our *goal-oriented ISAC access (GOIA)* with three benchmarks. 1) *push-oracle ISAC access (POIA)*: the first P UE with $V_u \geq \theta$, ordered by VoI, are able to access the push subframe with *no collision*; then, per-UE allocation and pull scheduling strategy are performed as GOIA. 2) *Goal-oriented communication access (GOCA)*, which perform the strategies of GOIA without enforcing localization, i.e., $Q_u^{\text{loc}} = 0, \forall u \in \mathcal{U}$; 3) *VoI-blind access (VIBA)*: UEs attempt transmission regardless of their VoI; the CPU solves the (14) by setting $V_u = 1, \forall u \in \mathcal{U}$.

Figs. 3a and 3b show the results vs. the VoI threshold, in terms of avg. total VoI of the scheduled UEs in the pull subframe, and avg. pull success rate, computed as the ratio between the amount of scheduled UEs within the pull subframe and $|\mathcal{S}|$, respectively. POIA performs best for $\theta \leq 0.25$, even with the lowest avg. pull access rate. Not being affected by collision, only the UEs carrying the highest VoI data are scheduled. VIBA performs the worst, expect when $\theta \approx 1$. Both GOIA and GOCA achieve a maximum for $\theta \approx 0.52$ corresponding to a push success rate of ≈ 0.63 . For $\theta > 0.52$, a fewer number of UEs attempt push access. Nevertheless, GOCA outperform GOIA, thanks to a pull access rate of

⁴The simulation code will be made available upon paper acceptance.

TABLE I: Simulation parameters.

Param.	Meaning	Value	Param.	Meaning	Value
L	no. APs	4	M	no. antenna	2
U	no. UEs	50	v_u	UE max speed	20 km/h
V_u	VoI	$\mathcal{U}(0, 1)$	B_u	obs. size	Geo(2^{10})
N_{rb}	num. RB	25	N_{ts}	no. slots	11
F	no. subcar.	12	T	OFDM sym.	7
Δ_F	subcar. spacing	30 kHz	T_{cp}	CP time	2.35 μs
N_p	push slots	2	P	push REs	50
N_q	pull slots	5	Q	pull REs	125
p_u	Tx. power	1 mW	σ_w^2	AWGN power	-95 dBm
θ	VoI thres.	0.7	ϵ	PEB constraint	1 m

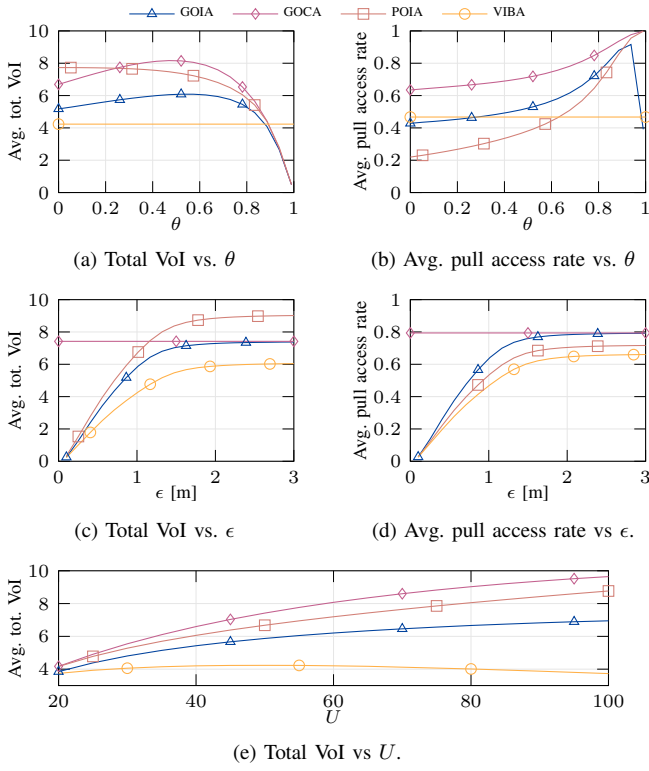


Fig. 3: Avg. performance.

≈ 0.72 against ≈ 0.53 . The reason is that the burden of resources of localization service is on average higher than the one required for communication due to the relatively high PEB constraints, and a loose bound (10).

Figs. 3c and 3d corroborate the previous statement, showing the results vs. the PEB constraint ϵ . When this value is loose (≈ 2.8 m) GOIA performs as well as GOCA, due to the reduced number of resources needed for localization—on avg. 90% of the time $Q_u^{\text{com}} \geq Q_u^{\text{loc}}$ $\epsilon = 2.8$ m, vs. 51% $\epsilon = 1$ m.

Finally, Fig. 3e shows the performance vs. U proving that the framework can improve the total VoI even when the UE are double than the pull REs P , while VoI-blind scheme fails. Further investigation must be done to assess the value of U maximizing the total VoI.

V. CONCLUSION AND FUTURE WORK

We presented a goal-oriented ISAC-enabled access framework for DT. By combining a VoI-aware push phase with a scheduled pull phase, our approach maximizes the per-frame total VoI, guaranteeing reliable communication and strict PEB. Simulation results demonstrate that the proposed GOIA outperforms VoI-blind schemes, while showing the performance gap due to ISAC. Future works will explore VoI estimation, tracking, and relax channel modeling assumptions.

APPENDIX

Implicitly taken w.r.t. $\mathbf{h}_{u,i}$, the gradients are:

$$\begin{aligned} \nabla_{\mathbf{x}_u} = & \sum_{\ell \in \mathcal{L}} \sqrt{\beta_{u,\ell}} e^{j\psi_{u,\ell}} (\mathbf{e}_\ell \otimes \nabla_{\mathbf{x}_u} \mathbf{f}_{u,\ell,i} \otimes \mathbf{a}_{u,\ell} \\ & + \mathbf{e}_\ell \otimes \mathbf{f}_{u,\ell,i} \otimes \nabla_{\mathbf{x}_u} \mathbf{a}_{u,\ell}) \in \mathbb{C}^{LFM \times 2}, \end{aligned}$$

$$\begin{aligned} \nabla_{\beta_u} = & \sum_{\ell \in \mathcal{L}} \frac{e^{j\psi_{u,\ell}}}{2\sqrt{\beta_{u,\ell}}} (\mathbf{e}_\ell \otimes \mathbf{f}_{u,\ell,i} \otimes \mathbf{a}_{u,\ell}) \mathbf{e}_\ell^\top \in \mathbb{C}^{LFM \times L}, \\ \nabla_{\psi_u} = & j \sum_{\ell \in \mathcal{L}} \sqrt{\beta_{u,\ell}} e^{j\psi_{u,\ell}} (\mathbf{e}_\ell \otimes \mathbf{f}_{u,\ell,i} \otimes \mathbf{a}_{u,\ell}) \mathbf{e}_\ell^\top \in \mathbb{C}^{LFM \times L}, \\ \nabla_{\delta\tau_u} = & \sum_{\ell \in \mathcal{L}} \sqrt{\beta_{u,\ell}} e^{j\psi_{u,\ell}} \mathbf{e}_\ell \otimes \nabla_{\delta\tau_u} \mathbf{f}_{u,\ell,i} \otimes \mathbf{a}_{u,\ell} \in \mathbb{C}^{LFM}, \end{aligned}$$

where $\nabla_{\mathbf{x}_u} \mathbf{f}_{u,\ell,i} = -j \frac{2\pi\Delta_F}{c} (\mathbf{n}_f \odot \mathbf{f}_{u,\ell,i}) \frac{(\mathbf{x}_u - \mathbf{b}_\ell)^\top}{\|\mathbf{x}_u - \mathbf{b}_\ell\|_2}$, $\nabla_{\mathbf{x}_u} \mathbf{a}_{u,\ell} = j \frac{2\pi}{\lambda} \mathbf{a}_{u,\ell} \mathbf{1}_2 \odot \frac{(\mathbf{B}_\ell - \mathbf{b}_\ell)^\top \mathbf{A}_\ell(\mathbf{x}_u)}{\|\mathbf{x}_u - \mathbf{b}_\ell\|_2}$, $\nabla_{\delta\tau_u} \mathbf{f}_{u,\ell,i} = -j 2\pi \Delta_F (\mathbf{n}_f \odot \mathbf{f}_{u,\ell,i})$, $\mathbf{n}_f = [f]_{f \in \mathcal{F}_i}^\top$, and $\mathbf{A}_\ell(\mathbf{x}_u) = \mathbf{I}_2 - \frac{(\mathbf{x}_u - \mathbf{b}_\ell)(\mathbf{x}_u - \mathbf{b}_\ell)^\top}{\|\mathbf{x}_u - \mathbf{b}_\ell\|_2^2}$.

REFERENCES

- [1] S. Mihai, M. Yaqoob, D. V. Hung *et al.*, “Digital twins: A survey on enabling technologies, challenges, trends and future prospects,” *IEEE Commun. Surveys Tuts.*, vol. 24, no. 4, pp. 2255–2291, Oct. 2022.
- [2] W. Liu, Y. Fu, Z. Shi, and H. Wang, “When digital twin meets 6G: Concepts, obstacles, and research prospects,” *IEEE Commun. Mag.*, vol. 63, no. 3, pp. 16–22, Mar. 2025.
- [3] A. Kaushik, R. Singh, S. Dayarathna *et al.*, “Toward integrated sensing and communications for 6G: Key enabling technologies, standardization, and challenges,” *IEEE Commun. Standards Mag.*, vol. 8, no. 2, pp. 52–59, Jun. 2024.
- [4] B. Li, X. Wang, Y. Xin, and E. Au, “Value of service maximization in integrated localization and communication system through joint resource allocation,” *IEEE Trans. Commun.*, vol. 71, no. 8, pp. 4957–4971, Aug. 2023.
- [5] W. Wang, D. Qiao, L. Yang *et al.*, “Optimal resource allocation design for wideband integrated sensing and communication systems,” *IEEE Trans. Wireless Commun.*, vol. 24, no. 3, pp. 2140–2156, Mar. 2025.
- [6] A. Topbas, C. Ari, O. Kaya, and E. Uysal, “Goal-oriented random access (gora),” *IEEE Wireless Commun. Lett.*, vol. 14, no. 8, pp. 2292–2296, Aug. 2025.
- [7] Z. Wang, V. W. Wong, and R. Schober, “Cooperative ISAC for joint localization and velocity estimation in Cell-Free MIMO systems,” *IEEE J. Sel Areas Commun.*, 2025.
- [8] S. Liesegang, S. Buzzi, and C. D’Andrea, “Scalable integrated sensing and communications for multi-target detection and tracking in cell-free massive MIMO: A unified framework,” *IEEE Trans. Commun.*, vol. 74, pp. 2777–2793, 2026.
- [9] F. Chiariotti and A. Zanella, “A theory of goal-oriented medium access: Protocol design and distributed bandit learning,” in *Proc. Conf. Comput. Commun. (INFOCOM)*. Tokyo, Japan: IEEE, May 2026.
- [10] P. Agheli, N. Pappas, and M. Kountouris, “Pull-based query scheduling for goal-oriented semantic communication,” *IEEE Trans. Commun.*, vol. 74, pp. 3845–3857, Jan. 2026.
- [11] S. R. Pandey, F. Saggese, J. Shiraishi *et al.*, “Medium access for push-pull data transmission in 6G wireless systems,” *IEEE Commun. Mag.*, 2026.
- [12] U. T. Demir, E. Björnson, and L. Sanguinetti, “Foundations of user-centric cell-free massive mimo,” *Foundations and Trends® in Signal Processing*, vol. 14, no. 3-4, pp. 162–472, 2021.
- [13] 3GPP, “NR: Study on new radio access technology Radio interface protocol aspects,” 3rd Generation Partnership Project (3GPP), Technical specification (TS) 38.804, 3 2017, version 14.0.0.
- [14] A. Omri, M. Shaqfeh, A. Ali, and H. Alnuweiri, “Synchronization Procedure in 5G NR Systems,” *IEEE Access*, vol. 7, pp. 41 286–41 295, 2019.
- [15] H. Wymeersch and G. Seco-Granados, “Radio localization and sensing—part II: State-of-the-art and challenges,” *IEEE Commun. Lett.*, vol. 26, no. 12, pp. 2821–2825, Dec. 2022.
- [16] K. Wu, J. Pegoraro, F. Meneghello *et al.*, “Sensing in bistatic ISAC systems with clock asynchronism: A signal processing perspective,” *IEEE Signal Process. Mag.*, vol. 41, no. 5, pp. 31–43, Sep. 2024.
- [17] H. Wymeersch and G. Seco-Granados, “Radio localization and sensing—part I: Fundamentals,” *IEEE Commun. Lett.*, vol. 26, no. 12, pp. 2816–2820, 2022.
- [18] S. M. Kay, *Fundamentals of statistical signal processing, volume I: Estimation theory*. Prentice Hall, Inc., Hoboken (NJ), USA, Apr. 1993.